IEEE Access
Multidisciplinary | Rapid Review | Open Access Journal

Received October 4, 2020, accepted October 15, 2020, date of publication October 19, 2020, date of current version October 28, 2020.

Digital Object Identifier 10.1109/ACCESS.2020.3031931

A Lossless Fiber Pressure Sensor Based on PDMS

CUI KAI, HONG YINGPING, SUI DANDAN, LIU WENYI, AND ZHANG HUIXIN
College of Instrumentation and Electronics, North University of China, Taiyuan 030051, China

Corresponding author: Hong Yingping (hongyingping@nuc.edu.cn)

This work was supported in part by the National Science Foundation for Outstanding Youth of China under Grant 51705475.

ABSTRACT Fiber optic pressure sensors have been widely used in recent decades. Most of the fiber optic pressure sensors use fiber gratings and Fabry-Perot cavity. However, they have the drawbacks of in achieving distributed sensing. In this paper, a lossless fiber pressure sensor based on a structure composed of two ratios of the polydimethylsiloxane (PDMS) and single-mode fiber is proposed. The PDMS has often been used as a flexible structural material. When the pressure is acting radially on the PDMS, the internal fiber is driven to produce an axial strain of a larger range, and the optical frequency domain reflectometer (OFDR) is used to demodulate the fiber strain. The experimental results prove that the designed sensor has a repeatable response with a sensitivity of 17.519 $\mu\varepsilon$/N within the range of 20 N (2548 kPa). The minimum pressure resolution and spatial resolution of the sensor can reach values of 0.5 N and 0.5 cm, respectively. Compared to a single ratio PDMS sensor, which has a non-linear response to the pressure, the range is increased by about 1.4 times. Based on the obtained results, the proposed sensor has application prospects in pressure sensors.

INDEX TERMS Fiber optic pressure sensor, polydimethylsiloxane (PDMS), pressure sensor.

I. INTRODUCTION

Fiber optic sensing technology, which is a new type of sensing technology, is sensitive to environmental parameters, such as temperature [1], strain, pressure [2], [3], and relative humidity [4], [5]. The optical fiber sensors (OFS), which have proven their advantages of anti-electromagnetic interference, lightweight, small size, high sensitivity, and simplicity in realizing multiplexing or distributed sensing, OFS are ideal in the diverse environment, such as oil well development, bridge maintenance, address exploration, and deep-sea exploration. At present, most of the fiber optic pressure sensors use fiber Bragg grating (FBG) pressure sensors [6]–[11] and Fabry-Perot (F-P) cavity pressure sensors [12]–[17]. Also, conventional fiber grating manufacturing methods include the phase template method and the amplitude template method. The phase template method is expensive and cannot be changed once it is manufactured, and is not suitable for the needs of research, design, and experimental analyses. Although there have been many types of amplitude templates, they all have disadvantages of large workload and long production time in mass production. Hence, the expensive and complicated FBG pressure sensor is inapplicable for mass production and a wide range of distributed pressure sensors. The optical fiber F-P sensors can be divided into intrinsic F-P interferometric (IFPI) sensors and extrinsic F-P interferometric (EFPI) sensors. The IFPI sensors are usually made of splicing fibers with a simple structure and good robustness. They are suitable for mass production and use, but they have disadvantages of high-pressure sensitivity and temperature cross-sensitivity. In contrast, the EFPI pressure sensors, which are formed between the reflective diaphragm and the end face of an optical fiber, has been widely used in different industries due to their small size, high sensitivity, fast response, and other advantages. However, the fabrication of the F-P cavity is complex, and it requires precise equipment and advanced technology, which significantly restricts its further development and application [18]–[20].

Polydimethylsiloxane (PDMS), which is a flexible polymer with various advantages, including excellent mechanical properties, good elasticity, lightweight, processability, chemical stability, and temperature sensitivity [21]–[25], has been widely used in capacitive pressure sensors, resistive pressure sensors, and microelectromechanical system (MEMS) sensors [26]–[28]. Due to the material properties of the PDMS, it can be made to have different structures by using simple methods [29], [30] and different characteristics by changing the mass ratio with the curing agent [31]. In this paper, a non-destructive optical fiber pressure sensor based on two ratios of the PDMS and an ordinary single-mode fiber is presented.

The associate editor coordinating the review of this manuscript and approving it for publication was Sukhdev Roy.

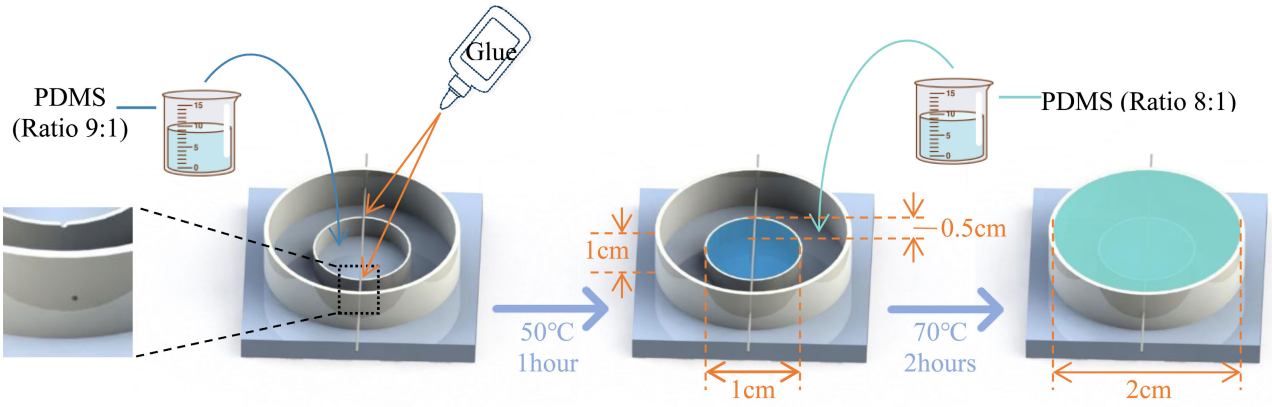

FIGURE 1. The sensor preparation process at two mass ratios; the PDMS of 8:1 was used as a flexible substrate, and PDMS of 9:1 was used as a buffer and protection material.

TABLE 1. Young's modulus of PDMS under ratio.

Quality ratio	Young's modulus (kg/m^3)
5:1	8.68×10^5
7.5:1	8.26×10^5
10:1	7.5×10^5
12.5:1	5.49×10^5
15:1	3.6×10^5

Compared to other types of fiber pressure sensors, this sensor has the advantages of a simple manufacturing process, and it compensates for the shortcomings of optical fibers of being fragile and unsuitable for exposure to the pressure field directly. By using unprocessed lossless optical fiber, and transforming its radial deformation to axial deformation, the transmission loss can be effectively reduced when strain is generated. Also, by using an optical frequency domain reflectometer (OFDR) for demodulation, fully distributed pressure measurement through a single fiber can be achieved.

II. MATERIALS AND METHODS

A. SENSOR MATERIALS

The preparation stage of the sensor is shown in Fig. 1. The shell of the sensor was constituted by a pedestal and two thin cylindrical walls having inner diameters of 1 cm and 2 cm. First, a magnetic stirrer was used to stir two mixed liquids, whose mass ratios of PDMS (Sylgard 184, Dow Corning, USA) to curing agent were 9:1 and 8:1. Young's moduli of PDMS under different ratios were shown in Table 1, the low specific gravity of the curing agent has the small Young's modulus. Therefore, it has high strain and sensitivity. The typical PDMS ratio is 5:1–10:1. However, the sensor with a ratio of 10:1 has a small range about 10N, at the same time with large strain residual and hysteresis. Therefore, the ratio of 9:1 and 8:1 was finally selected.

Then, the single-mode fiber in the sequence was pulled through two fixed holes of the shell, and α-cyanoethyl acrylate was used to treat the straightened fiber in order to prevent the tension of the PDMS solution from bending the optical fiber. The two mixtures were left to stand until the bubbles disappeared, and then the 9:1 PDMS liquid was slowly poured into the smaller cylinder. Next, the sensor shell was placed horizontally at 50 °C for 1 hour to pre-cure. After taking out the shell and cooling it, the 8:1 PDMS liquid was poured into a larger cylinder to fill the entire container. Finally, the pressure sensor was prepared by placing the sensor shell horizontally at 70 °C for 2 hours.

B. WORKING PRINCIPLE

A sensor produces radial elastic deformation when external pressure acts on the PDMS, causing a larger range of elastic squeezing deformation inside the sensor to drive the optical fiber to produce a large range of axial elastic deformation, thus increasing the optical sensitivity of the fiber. At the same time, flexible PDMS wraps the fragile and bare optical fiber, which can significantly improve the environmental suitability of the optical fiber sensor [32].

When a laser is transmitted along a section of a fiber, a backscatter occurs due to structural defects of fine particles or pores during the cooling process of the optical fiber manufacturing. This inevitable and specific reflection is called Rayleigh backscattering along a fiber. The original path between the Rayleigh scattering position ξ_L in the fiber produces a relative displacement $\Delta\xi_L$ when the stress acts on the sensor.

The cross-sectional view of a sensor is shown in Fig. 2, where it can be seen that sensor can be divided into two parts: (1) a PDMS part with the mass ratio of 8:1, and high rigidity and small elastic modulus, which can be approximated to a rigid body under small deformations; and (2) a sensor with the mass ratio of 9:1 and higher elastic modulus volume, and it can be regarded as an elastic object. Based on Hooke's Law, an effective strain can be defined as:

$$\Delta\varepsilon_{eff} = \frac{\Delta\zeta_L}{\zeta_L} = \frac{\Delta F}{k_L\zeta_L}, \tag{1}$$

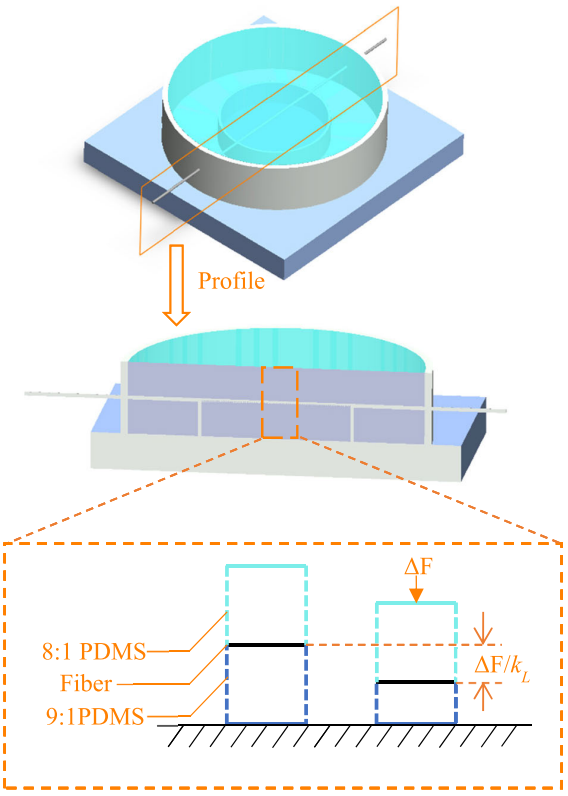

FIGURE 2. The equivalent model of the sensor with an optical fiber profile and local deformation under force.

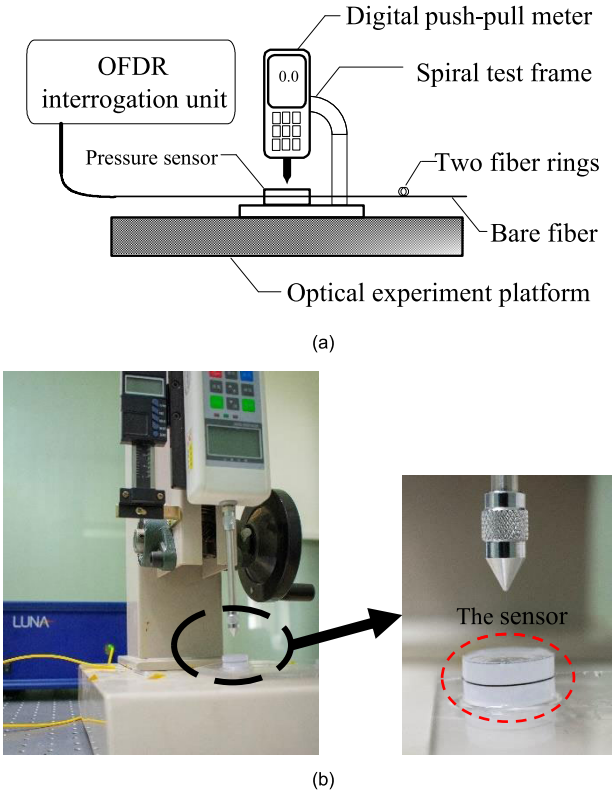

FIGURE 3. (a) Schematic diagram of the experimental system; (b) Images of the experimental system.

where k_L denotes the PDMS equivalent elastic coefficient, and ΔF denotes the pressure change. In this paper, $\Delta\varepsilon_{eff}$ denotes the fiber strain, and it is measured using the Optical Frequency Domain Reflectometry (OFDR). The OFDR measurement system uses a coherent detection method. The light emitted by a tunable wavelength laser is divided into two beams by the fiber coupler, of which one is reflected by a mirror and enters the photodetector as reference light, and another beam is caused by Rayleigh backscattering and reflected to the photodetector (PD), and it is used as a signal light. The two output beams form interference fringes in the spectral domain at the PD, and the position and strain information of the fiber strain point can be obtained by Fourier transform.

C. METHOD OF MEASUREMENT

The pressure sensor configuration and the experimental setup used in the characterization experiments are shown in Fig 3. The backlight reflectometer (Luna Corporation, OBR4600, USA) was used as a demodulation device. The laptop computer (DELL, Precision 5520) was used to demodulate the single measurement data. The spiral test frame was used to fix load systems and sensors. The digital push-pull force meter (Sando Instruments, China) was used to apply pressure with a force area of a radius of 0.5 mm. The spiral test frame and force meter constituted the pressure characterization system. When the signal light was transmitted along the optical fiber, the end face reflection was generated at the end of the optical fiber to return to the OFDR, which then interfered with the measurement signal. Two fiber rings with a diameter of 5 mm could effectively suppress the interference signal generated by the end face due to its large loss.

In order to further verify that the optical fiber pressure sensor can be applied to fully distributed sensing and achieve sufficient sensitivity and pressure test ranges, the sensing length and sensing unit interval were both set to 0.5 cm. The sensing interval was set to 0.5 m because this value was convenient to locate the load center and reduce the demodulation time of the computer. The force from the pressure characterization system acted on the sensor center. Because of the temperature-sensitive nature of the PDMS, the experiment was conducted at 25°C to avoid the interference of temperature fluctuations.

III. RESULTS AND DISCUSSION

The OFDR Rayleigh backscattering data obtained by the pressure sensor configuration presented in Fig. 4 was acquired under pressure from the characterization system at 27°C. Under the selected configuration and a single-point pressure, the pressure response curve had a single peak, indicating that the sensor had a good response to the pressure. The measurement and demodulation time of the entire 0.5-m fiber by the computer was about 2 s. Most of this time was used to demodulate the data, while the measurement process took less

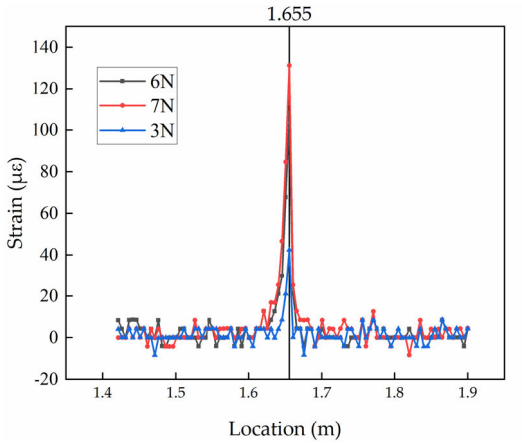

FIGURE 4. The OFDR Rayleigh backscattering results in the pressure sensor range from 1.42 m to 1.9m including 3 times.

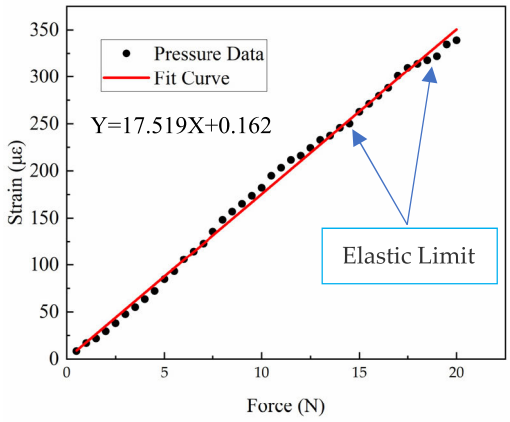

FIGURE 5. The OFDR Rayleigh backscattering data of the pressure sensor (range 0–20 N, step 0.5 N).

than one second. The strain-spatial distribution measurement results under different loads were analyzed; the measured peaks were all at 165.5 cm, and the position coordinates' intervals were 0.5 cm. The load center remained unchanged in the experiments, which was consistent with the measurement results under the current spatial resolution setting. Also, it was verified that the spatial resolution of the sensing system reached a value of 0.5 cm.

The measurement results included system noise, whose absolute value was mainly in the range of 0–5 $\mu\varepsilon$, and the maximum value was less than 9 $\mu\varepsilon$. The noise was mainly generated due to the high sensitivity of OFDR measurement, making the fiber sensitive to slight vibrations and temperature fluctuations in the measurement environment. Part of the noise originated from the measurement error of the OFDR itself, and this part could not be suppressed by simply improving the optical path. Therefore, in order to reduce the influence of environmental noise on the measurement results in the experiment, the suspended part of the fiber on the optical experiment platform was fixed by polyimide tape. The results showed that the frequency of environmental noise was significantly reduced, but its amplitude was not suppressed.

The experimental results of the pressure are shown in Fig. 5. The experiment results showed that the strain value of the optical fiber was positively correlated with the applied pressure, and its linear fitting degree reached a value of 0.996. The force sensing range of the sensor was 20 N (2548 kPa), the minimum resolution was 0.5 N (64kPa), and the sensitivity was 17.519 $\mu\varepsilon$/N.

In a single full-scale measurement, when the force was about 14.5 N or 19 N, the strain value not only did not show a good correlation with the force increase but also showed zero growth. This fluctuation can be explained as follows. The fiber was sandwiched between two types of PDMSs having different ratios and elastic limits, which meant that the load at 14.5 N or 19 N reached the elastic limit of the two materials. In that state, the PDMS produced a small amount of plastic deformation, resulting in the obtained measurement results that are presented above. In order to verify the conjecture,

TABLE 2. Strain residual values for four pressure values.

Force (N)	Strain (με)			Strain recovery time (s)
	No1	No2	No3	
14	0.254	0.102	-0.203	0
14.5	-12.542	-8.231	-12.534	12
18.5	-16.452	-16.264	-15.981	13
19	-25.213	-25.143	-29.427	18

the additional experiment was conducted. Loads of 14 N, 14.5 N, 18.5 N, and 19 N were respectively applied to the sensor, and then immediately removed. The residual strain values of the sensor after removing the corresponding loads were recorded, and they are given in Table 2.

As presented in Table 1, the loads of 14.5 N and 19 N reached the elastic deformation limit of the two materials. In such a situation, the material will undergo plastic deformation, leaving residual strain after removing the load. This small plastic deformation can be recovered in a short time, so although it will affect the sensor linearity, it will not limit the sensor range.

The repeatability of the sensor was also verified at 27°C, and obtained results are shown in Fig. 6. The result in Fig. 6 shows that the pressure sensor has good repeatability in the environment with a constant temperature. However, the proposed structure has a limitation. Namely, the PDMS lost its elasticity after several tests, which could be because the load exceeded the elastic limit of PDMS and caused some irreversible damage to the PDMS structure.

The performance comparison of the presented sensor and the sensor that uses only 1:9 PDMS as a base is shown in Fig. 7. The sensing range of the pressure sensor using a single ratio was 14 N (1783kPa), and the response to the pressure was closer to a quadratic curve and had higher sensitivity. The pressure sensor using the compound PDMS had a higher sensing range (2 times) and a linear response

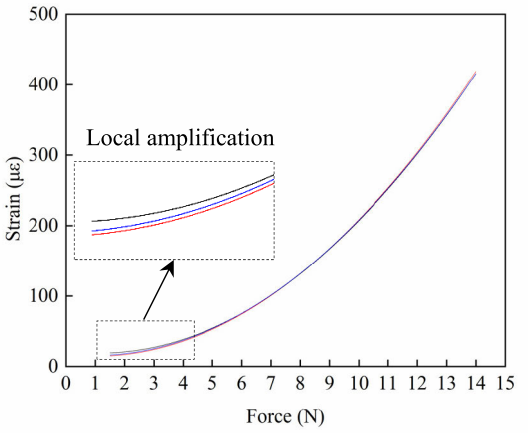

FIGURE 6. Sensor repeatability measurement result of three times (range 0–20 N, step 0.5 N).

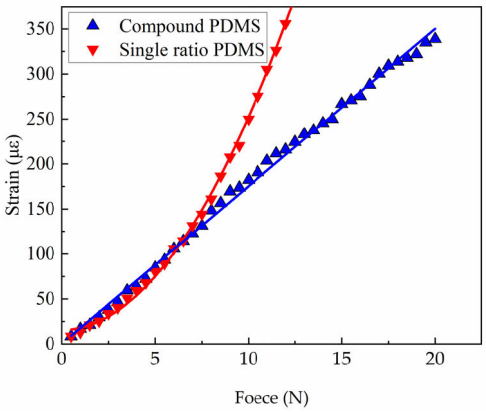

FIGURE 8. Repeatability measurement fitting curve of the single-ratio sensor (9:1).

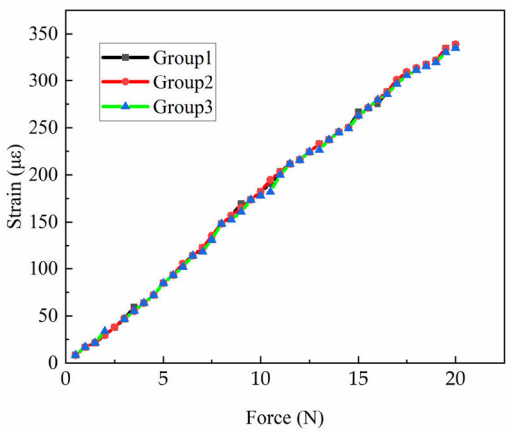

FIGURE 7. The comparison between the single-ratio PDMS and the compound PDMS.

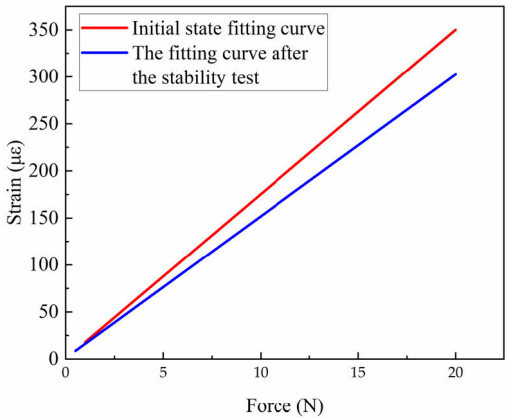

FIGURE 9. Diagram of stability experiment results.

to pressure than the sensor that uses only 1:9 PDMS as a base, so it is more suitable to be used as a fiber pressure sensor.

The repeatability test result of the single-ratio sensor is shown in Fig. 8, where it can be seen that the three sets of fitting curves reached a high degree of consistency, but the coincidence of the fitting curves was relatively poor under low-load conditions. The force feedback value was zero when the load was less than 1.5 N. The 9:1 PDMS was a soft flexible material that had high buffering and absorption capacity for pressure. When the load was less than 1.5 N, the stress was not transmitted to the surface of the fiber under test. The method of applying pre-stress can be used to eliminate the measurement dead zone of the sensor 0–1.5 N. The results show that the repeatability measurement results of the sensor were good and had good stability.

The stability of the presented sensor was also investigated experimentally. The obtained experimental results of the fitting curve are shown in Fig. 9. The results showed that the sensor had good stability. However, after about 40 tests over 48 hours, the aging of PDMS and the damage of the internal structure caused the decrease of the sensitivity from 17.519 $\mu\varepsilon$/N to 16.646 $\mu\varepsilon$/N. It still had good linearity with a fitting degree of 0.996.

Finally, the temperature and relative humidity sensitivity property of the presented sensor were investigated. The sensor and the pressure characterization system were placed in a high and low temperature damp heat test box with a rapid temperature change (SDJS701B, Chongqing Sida Test Equipment Co. LTD, China). The experimental results showed that the sensor was insensitive to humidity but sensitive to temperature. In the temperature range of 20–50 °C, the sensor produced zero temperature drift with the temperature change, but the sensitivity and linearity of the sensor did not change under constant temperature conditions. At the reference temperature of 20 °C, the changing curve of the zero strain with the temperature is shown in Fig. 10, where it can be seen that there was a linear relationship between temperature and strain, and the sensitivity was about 7.460 $\mu\varepsilon$/°C. Therefore, the pressure value can be temperature compensated by measuring the current ambient temperature.

The comparison of different types of fiber-optic pressure sensors is given in Table 3. The fiber optic pressure sensor proposed in this paper had reached the pressure sensing range

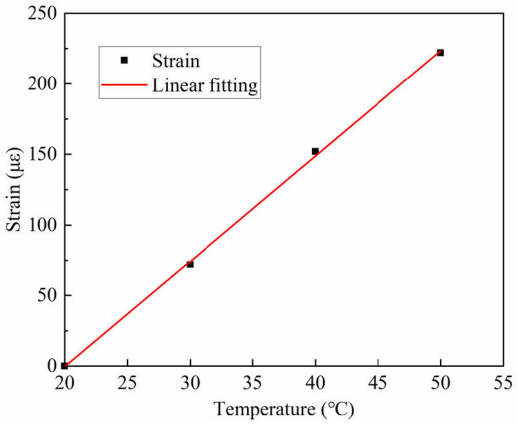

FIGURE 10. **The zero-strain value dependence on the temperature change in the temperature range of 20–50 °C.**

TABLE 3. **Comparison of different fiber optic pressure sensors.**

Reference	Pressure range	Sensor type	Sensitivity
[6]	330 kPa	Fiber grating sensor	0.65 pm/kPa
[19]	900 kPa	F-P cavity fiber optic sensing	59.39 pm/kPa
[33]	10 kPa	SMF in an engineered cable	30 GHz/kPa
This work	2548 kPa	SMF in PDMS	0.14 με/kPa

of the mainstream pressure sensors. At the same time, compared with other pressure sensors, it has simple manufacturing process.

IV. CONCLUSION

In this paper, a pressure sensor based on two ratios of the PDMS is proposed for pressure measurements. The sensing material preparation, structure design, and signal demodulation method are presented. The designed sensor is analyzed in terms of linearity, spatial resolution, and repeatability. In addition, the sensor is compared with a single-ratio PDMS sensor. Finally, the pressure sensor is successfully used to conduct pressure measurement. The results show that the proposed sensor can be successfully used in pressure measurements, and it has potential applications in pressure sensing.

Future studies will focus on distributed pressure sensing and improvement of the PDMS structure to achieve greater pressure ranges and be used in more stable applications.

REFERENCES

[1] Z. Zhou, Z. Li, N. Tang, J. Sun, K. Han, and Z. Wang, "On-line temperature measurement of fiber Bragg gratings inside a fiber laser," *Opt. Fiber Technol.*, vol. 45, pp. 137–140, Nov. 2018, doi: 10.1016/j.yofte.2018.07.009.

[2] B. Zhou, "Highly sensitive small pressure monitoring using hyperelastic silicone-cladding/silica-core composite optical fiber," *IEEE Photon. J.*, vol. 9, no. 6, Dec. 2017, Art. no. 6805208, doi: 10.1109/JPHOT.2017.2779605.

[3] X. Li, H. Zhang, C. Qian, Y. Ou, R. Shen, and H. Xiao, "A new type of structure of optical fiber pressure sensor based on polarization modulation," *Opt. Lasers Eng.*, vol. 130, Jul. 2020, Art. no. 106095, doi: 10.1016/j.optlaseng.2020.106095.

[4] P. J. Thomas and J. O. Hellevang, "A fully distributed fibre optic sensor for relative humidity measurements," *Sens. Actuators B, Chem.*, vol. 247, pp. 284–289, Aug. 2017, doi: 10.1016/j.snb.2017.02.027.

[5] P. J. Thomas and J. O. Hellevang, "A high response polyimide fiber optic sensor for distributed humidity measurements," *Sens. Actuators B, Chem.*, vol. 270, pp. 417–423, Oct. 2018, doi: 10.1016/j.snb.2018.05.011.

[6] L. Zhang, H. Lin, C. Du, X. Liu, X. Lu, X. Deng, and L. Cui, "Performance investigation on pressure sensing from fiber Bragg grating loop ring-down cavity," *Opt. Commun.*, vol. 469, Aug. 2020, Art. no. 125759, doi: 10.1016/j.optcom.2020.125759.

[7] A. G. Leal-Junior, A. Frizera, and C. Marques, "Thermal and mechanical analyses of fiber Bragg gratings-embedded polymer diaphragms," *IEEE Photon. Technol. Lett.*, vol. 32, no. 11, pp. 623–626, Jun. 1, 2020, doi: 10.1109/LPT.2020.2988554.

[8] L. Liu, Y. Li, Y. He, F. Li, and Y. Liu, "Membrane-based fiber Bragg grating pressure sensor with high sensitivity," *Microw. Opt. Technol. Lett.*, vol. 51, no. 5, pp. 1279–1281, May 2009, doi: 10.1002/mop.24335.

[9] P.-L. Ko, K.-C. Chuang, and C.-C. Ma, "A fiber Bragg grating-based thin-film sensor for measuring dynamic water pressure," *IEEE Sensors J.*, vol. 18, no. 18, pp. 7383–7391, Sep. 2018, doi: 10.1109/JSEN.2018.2857561.

[10] H. Ahmad, S. W. Harun, W. Y. Chong, M. Z. Zulkifli, M. M. M. Thant, Z. Yusof, and P. Poopalan, "High-sensitivity pressure sensor using a polymer-embedded FBG," *Microw. Opt. Technol. Lett.*, vol. 50, no. 1, pp. 60–61, Jan. 2008, doi: 10.1002/mop.23021.

[11] V. R. Pachava, S. Kamineni, S. S. Madhuvarasu, K. Putha, and V. R. Mamidi, "FBG based high sensitive pressure sensor and its low-cost interrogation system with enhanced resolution," *Photonic Sensors*, vol. 5, no. 4, pp. 321–329, Dec. 2015, doi: 10.1007/s13320-015-0259-7.

[12] D. Fu, X. Liu, J. Shang, W. Sun, and Y. Liu, "A simple, highly sensitive fiber sensor for simultaneous measurement of pressure and temperature," *IEEE Photon. Technol. Lett.*, vol. 32, no. 13, pp. 747–750, Jul. 1, 2020, doi: 10.1109/LPT.2020.2993836.

[13] W. Ma, Y. Jiang, J. Hu, L. Jiang, T. Zhang, and T. Zhang, "Microelectromechanical system-based, high-finesse, optical fiber Fabry–Pérot interferometric pressure sensors," *Sens. Actuators A, Phys.*, vol. 302, Feb. 2020, Art. no. 111795, doi: 10.1016/j.sna.2019.111795.

[14] K. Chen, "Simultaneous measurement of acoustic pressure and temperature using a Fabry–Pérot interferometric fiber-optic cantilever sensor," *Opt. Express*, vol. 28, no. 10, pp. 15050–15061, May 2020, doi: 10.1364/OE.387195.

[15] H. Chen, "Fiber optic pressure sensor based on a single-mode fiber F–P cavity," *Measurement*, vol. 43, no. 3, pp. 370–374, Apr. 2010, doi: 10.1016/j.measurement.2009.12.002.

[16] J. Shi, "Remote Gas pressure sensor based on fiber ring laser embedded with Fabry–Pérot interferometer and Sagnac loop," *IEEE Photon. J.*, vol. 8, no. 5, Oct. 2016, Art. no. 6804408, doi: 10.1109/JPHOT.2016.2605460.

[17] C. Luo, X. Liu, J. Liu, J. Shen, H. Li, S. Zhang, J. Hu, Q. Zhang, G. Wang, and M. Huang, "An optimized PDMS thin film immersed Fabry–Pérot fiber optic pressure sensor for sensitivity enhancement," *Coatings*, vol. 9, no. 5, p. 290, Apr. 2019, doi: 10.3390/coatings9050290.

[18] Y. Li, W. Zhang, Z. Wang, H. Xu, J. Han, and F. Li, "Low-cost and miniature all-silica Fabry–Pérot pressure sensor for intracranial pressure measurement," *Chin. Opt. Lett.*, vol. 12, no. 11, Nov. 2014, Art. no. 111401, doi: 10.3788/COL201412.111401.

[19] M. F. Domingues, C. A. Rodriguez, J. Martins, C. Tavares, C. Marques, N. Alberto, P. André, and P. Antunes, "Cost-effective optical fiber pressure sensor based on intrinsic Fabry–Pérot interferometric micro-cavities," *Opt. Fiber Technol.*, vol. 42, pp. 56–62, May 2018, doi: 10.1016/j.yofte.2018.02.016.

[20] R. A. Pérez Herrera, S. Novais, M. Bravo, D. Leandro, S. Silva, O. Frazao, and M. Lopez-Amo, "Multiplexing optical fiber Fabry–Pérot interferometers based on air-microcavities," *Proc. SPIE*, vol. 11199, Aug. 2019, Art. no. 1119925, doi: 10.1117/12.2540150.

[21] J. Paek, Q. Li, I. Cho, and J. Kim, "Minimally intrusive optical microstrain sensing in bulk elastomer using embedded Fabry–Pérot etalon," *Micromachines*, vol. 7, no. 4, p. 61, Apr. 2016, doi: 10.3390/mi7040061.

[22] X. Zhang, R. Chai, H. Wang, and X. Ye, "A plantar pressure sensing system with balancing sensitivity based on tailored MWCNTs/PDMS composites," *Micromachines*, vol. 9, no. 9, p. 466, Sep. 2018, doi: 10.3390/mi9090466.

[23] A. Kulkarni, H. Kim, J. Choi, and T. Kim, "A novel approach to use of elastomer for monitoring of pressure using plastic optical fiber," *Rev. Sci. Instrum.*, vol. 81, no. 4, Apr. 2010, Art. no. 045108, doi: 10.1063/1.3386588.
[24] Y. Kim, S. Jang, and J. H. Oh, "Fabrication of highly sensitive capacitive pressure sensors with porous PDMS dielectric layer via microwave treatment," *Microelectron. Eng.*, vol. 215, Jul. 2019, Art. no. 111002, doi: 10.1016/j.mee.2019.111002.
[25] M. Xu, Y. Gao, G. Yu, C. Lu, J. Tan, and F. Xuan, "Flexible pressure sensor using carbon nanotube-wrapped polydimethylsiloxane microspheres for tactile sensing," *Sens. Actuators A, Phys.*, vol. 284, pp. 260–265, Dec. 2018, doi: 10.1016/j.sna.2018.10.040.
[26] A. P. Gerratt, I. Penskiy, and S. Bergbreiter, "*In situ* characterization of PDMS in SOI-MEMS," *J. Micromech. Microeng.*, vol. 23, no. 4, Apr. 2013, Art. no. 045003, doi: 10.1088/0960-1317/23/4/045003.
[27] J. Ruhhammer, M. Zens, F. Goldschmidtboeing, A. Seifert, and P. Woias, "Highly elastic conductive polymeric MEMS," *Sci. Technol. Adv. Mater.*, vol. 16, no. 1, Feb. 2015, Art. no. 015003, doi: 10.1088/1468-6996/16/1/015003.
[28] L.-J. Yang, H.-H. Wang, P.-C. Yang, Y.-C. Chung, and T.-S. Sheu, "New packaging method using PDMS for piezoresistive pressure sensors," *Sensors Mater.*, vol. 19, no. 7, pp. 391–403, 2007.
[29] X. Zhao, W. Xu, W. Yi, and Y. Peng, "A flexible and highly pressure-sensitive PDMS sponge based on silver nanoparticles decorated reduced graphene oxide composite," *Sens. Actuators A, Phys.*, vol. 291, pp. 23–31, Jun. 2019, doi: 10.1016/j.sna.2019.03.038.
[30] Q. Lü, H. Cao, X. Song, H. Yan, Z. Gan, and S. Liu, "Improved electrical resistance-pressure strain sensitivity of carbon nanotube network/polydimethylsiloxane composite using filtration and transfer process," *Chin. Sci. Bull.*, vol. 55, no. 3, pp. 326–330, Jan. 2010, doi: 10.1007/s11434-009-0562-z.
[31] Y. Peng, S. Xiao, J. Yang, J. Lin, W. Yuan, W. Gu, X. Wu, and Z. Cui, "The elastic microstructures of inkjet printed polydimethylsiloxane as the patterned dielectric layer for pressure sensors," *Appl. Phys. Lett.*, vol. 110, no. 26, Jun. 2017, Art. no. 261904, doi: 10.1063/1.4990528.
[32] J. Bunyan and S. Tawfick, "Mechanical behavior of PDMS at low pressure," *Mater. Res. Express*, vol. 4, no. 7, Jul. 2017, Art. no. 075306, doi: 10.1088/2053-1591/aa7d8a.
[33] L. Schenato, A. Pasuto, A. Galtarossa, and L. Palmieri, "An optical fiber distributed pressure sensing cable with pa-sensitivity and enhanced spatial resolution," *IEEE Sensors J.*, vol. 20, no. 11, pp. 5900–5908, Jun. 2020, doi: 10.1109/JSEN.2020.2972057.

CUI KAI was born in Shanxi, China, in 1995. He received the bachelor's degree from the School of Instruments and Electronics, North University of China, in 2014. He is currently a Graduate Student with the North University of China. His current research interests include optical fiber sensors for pressure and distributed measurements.

HONG YINGPING was born in Shanxi, China, in 1984. He is currently an Associate Professor with the Institute of Instrumentation and Electronics, North University of China. His main research interests include testing technology and instrument research in extreme environments.

SUI DANDAN was born in Heilongjiang, China, in 1995. She received the bachelor's degree from the School of Instruments and Electronics, North University of China, in 2014. She is currently a Graduate Student with the North University of China. Her research interests include optical fiber sensors for pressure and distributed measurements.

LIU WENYI was born in Shanxi, China, in 1970. He is currently a Full Professor with the Institute of Instrumentation and Electronics, North University of China. His current research interests include distributed data recording systems, wireless sensor networks, embedded systems, data encryption, multifunctional structure, wireless sensor networks, special optical sensors, and new high-speed data transmission bus development.

ZHANG HUIXIN was born in Heilongjiang, China, in 1980. He is currently an Associate Professor with the Institute of Instrumentation and Electronics, North University of China. His research interests include flexible distributed optical fiber sensing technology and testing technology of high overload, large capacity, and high-speed solid-state storage.